

PAA/imidazol-based proton conducting polymer electrolytes

A. Bozkurt^{a,*}, W.H. Meyer^b, G. Wegner^b

^a Department of Chemistry, Fatih University, 34900 Buyukcekmece, Istanbul, Turkey

^b Max-Planck-Institut für Polymerforschung, Ackermannweg 10, D-55128 Mainz, Germany

Received 7 December 2002; received in revised form 1 April 2003; accepted 14 April 2003

Abstract

Anhydrous proton conducting polymer electrolytes have been prepared by entrapping imidazol (Im) in polyacrylic acid (PAA) with various stoichiometric ratios, x , to form PAA x Im (x is the number of moles of Im per polymer repeat unit). Polymer electrolytes, PAA x Im (with $x = 0.5$ and 1) can be cast into transparent, homogeneous films. FT-IR results indicate the protonation of imidazol. Thermogravimetric analysis (TG) illustrates that these blends are chemically stable up to about 160 °C. Differential scanning calorimetry (DSC) shows that glass transition temperature decrease from 57 °C for $x = 0.5$ to 35 °C for $x = 1$. The dc conductivity increases with x and temperature reaching $\sim 10^{-3}$ S/cm for $x = 1$ at 120 °C.

© 2003 Elsevier B.V. All rights reserved.

Keywords: Poly (acrylic acid); Imidazol; Proton conductor; Thermal properties

1. Introduction

Proton conducting polymer electrolytes have attracted much attention with the development of perfluorinated sulfonic membranes due to their application in various electrochemical devices such as fuel cells. The transport properties of those membranes are largely depending of water content and can be useful below the dew point of water [1]. It is also well established that anhydrous proton conducting polymer electrolytes were obtained by doping of polymers bearing basic units such as amide, imine, ether with strong acids, i.e. H₃PO₄ or H₂SO₄ [2–5]. In these blends strong acids act as both proton donor and plasticizer [6,7]. Recently, neutral (or basic) proton conducting polymer electrolytes have already been announced as they are likely to be more stable in the presence of electrode materials [8]. In such membranes the basic dopant enhanced proton vacancy type conduction. Although the formation of protonic defects is necessary for proton conduction, the reported conductivities are relatively low. Heterocycles such as imidazol have been reported to be promising in that respect. Their nitrogen sides act as strong proton acceptors thus forming protonic charge carriers. Isometric geometry of molecules are advantageous for extended local dynamics and their protonated and unprotonated nitrogen functions may act as donors and

acceptors in proton transfer reactions [9]. Previously, Kreuer et al, created protonic defects by chemically modifying the heterocycles [9]. In addition, polybenzimidazol/H₃PO₄ system was modified with imidazol but it was mentioned that imidazolium salt does not improve the conductivity of the membranes [10]. Very recently, proton conductivity in imidazol which was immobilized via flexible spacers has been demonstrated [11]. In the present work, proton conducting polymer electrolytes based on PAA/Im are reported. The synthesis of these materials and their thermal and conductivity properties are discussed.

2. Experimental

2.1. Materials preparation

Polyacrylic acid (PAA) was prepared by conventional radical polymerization of acrylic acid (Merk) at 80 °C in benzene with azobisisobutyronitrile (AIBN) as initiator [12]. Aqueous solution of the polymer was dialyzed using 1000 molecular weight cut off membrane and freeze dried. A stoichiometric amount of imidazol (Aldrich) and PAA was neutralized in water and the resulting mixture was stirred for several days to make it homogeneous. Solutions with x ranging from 0.5 to 3.0 were prepared where x is the number of moles of imidazol per moles of polymer repeat unit. From the solutions films were cast in a polished PTFE plates, and the solvent was carefully evaporated over P₂O₅ and further

* Corresponding author. Fax: +90-212-8890832.
E-mail address: bozkurt@fatih.edu.tr (A. Bozkurt).

dried under vacuum at 60 °C. Transparent and homogeneous films were obtained for $x = 0.5$ and 1, however, at higher x values, i.e. $x > 1$, phase separated mixtures were obtained.

2.2. Characterizations

FT-IR spectra of the samples were recorded by casting of thin sample film on a silicon wafer. The IR spectra of the samples were recorded with a Nicolet 730 spectrophotometer.

Thermal stabilities of the materials were investigated by thermogravimetric analysis with a Mettler TG-50. The samples (~10 mg) were heated from room temperature to 700 °C with a rate of 10 °C/min under N₂ atmosphere.

DSC data were obtained between –50 and 130 °C using a Mettler DSC TA 3000 scanning calorimeter. The samples were loaded into aluminum pans (10–15 mg) and samples were heated to desired temperature with a rate of 10 °C/min. The second heating curves were evaluated.

The ac conductivities of PAAxIm samples were determined with an Novocontrol dielectric spectrometer in the frequency range from 10⁻² to 10⁷ Hz and in the temperature regime from –50 to 150 °C. The film samples were placed between platinum electrodes and their conductivities

were measured with 10 K intervals. The temperature was controlled with Novocontrol cryosystem which is applicable between –150 and 500 °C with a precision of 0.01 °C.

3. Results and discussion

3.1. Polymer–imidazol interactions

FT-IR spectra of the homopolymer and blends are represented in Fig. 1. A strong absorption at 1707 cm⁻¹ belongs to C=O stretching of carboxylic acid group of the homopolymer. The same group shows a medium peak at 1250 cm⁻¹ corresponding to in plane deformation of C–O–H and at 1165 cm⁻¹ to –(C–O)H stretching. After blending the polymer with imidazol a new strong peak appears at 1557 cm⁻¹ and the intensity of the carbonyl stretching at 1707 cm⁻¹ decreases. These occur by the transfer of the acidic proton of the carboxylic acid to the “free” nitrogen side of imidazol to form imidazolium ion. Then the carboxylic acid units, C=O and C–O, are replaced by two carbon oxygen bonds which are intermediate force constants between them. These two bands are strongly coupled, resulting in strong asymmetric stretching of –CO₂⁻ at 1557 cm⁻¹. Ring stretching of the

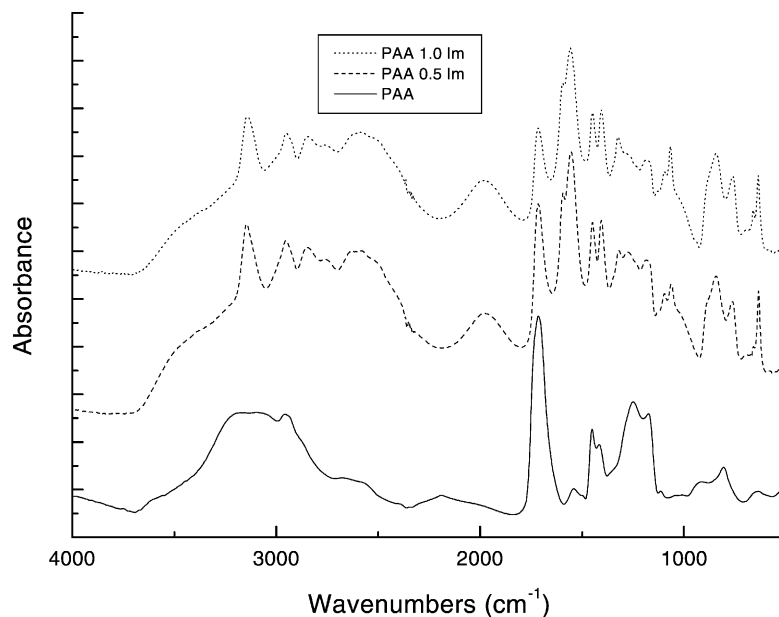


Fig. 1. FT-IR spectra of pure PAA, PAA0.5Im and PAA1.0Im.

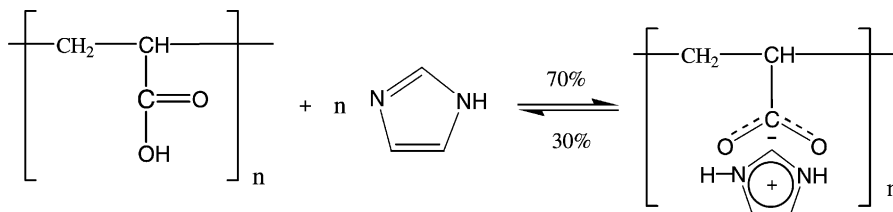


Fig. 2. Illustration of the protonation of imidazol upon blending with PAA.

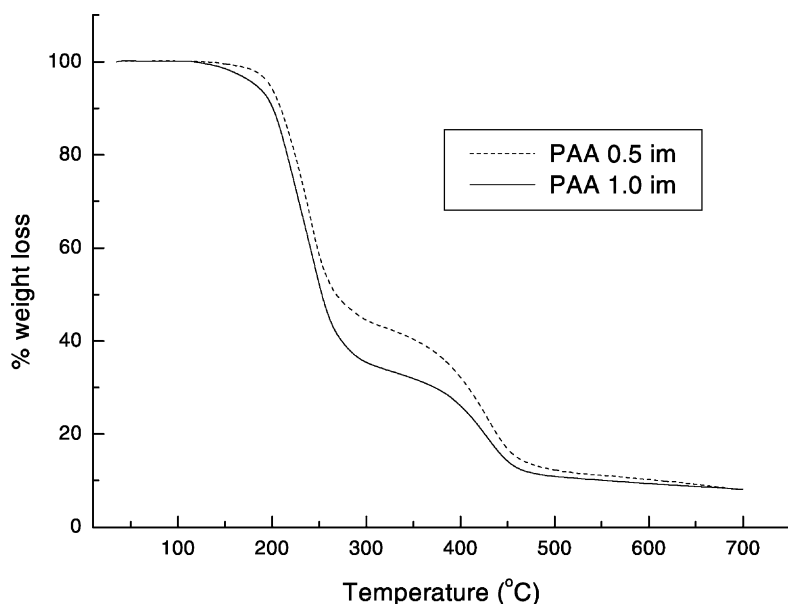


Fig. 3. TG curves of PAA0.5Im and PAA1.0Im recorded under N_2 atmosphere with a heating rate of 10 K/min.

imidazolium ion at 1595 cm^{-1} is masked by the CO_2^- absorption. Fig. 2 represents the percent conversion of imidazol to imidazolium ion which is obtained from carbonyl stretching for $x = 1$. The percent protonation of the blends was found to be $\sim 33\%$ for $x = 0.5$ and $\sim 70\%$ for $x = 1.0$. The intensity of N–H stretching peak at 3140 cm^{-1} is also increased due to protonation.

3.2. Thermal analysis

Thermogravimetric analyses (TG) were performed under nitrogen atmosphere. The samples were dried 2 days un-

der vacuum at 60°C prior to measurement. For anhydrous $\text{PAA}x\text{Im}$ complexes the initial weight reduction starts at 180°C for $x = 0.5$ and at 160°C for $x = 1$ (Fig. 3). The weight loss above these temperatures can be attributed to evaporation of dopant and followed with decomposition of the blends above 200°C .

DSC thermograms of $\text{PAA}x\text{Im}$ are shown in Fig. 4. The T_g of the homopolymer is 105°C shifted to 35°C for $x = 1$ because of the plasticization effect of dopant which was explained in our previous work [7]. It is clearly seen that one phase model is reasonable assumption for anhydrous $\text{PAA}x\text{Im}$ blends.

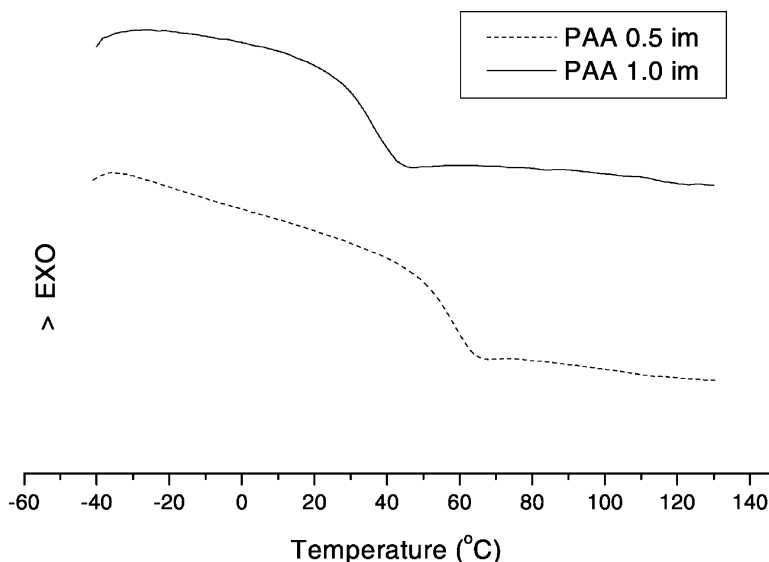


Fig. 4. DSC curves of PAA0.5Im and PAA1.0Im recorded under N_2 atmosphere with a heating rate of 10 K/min.

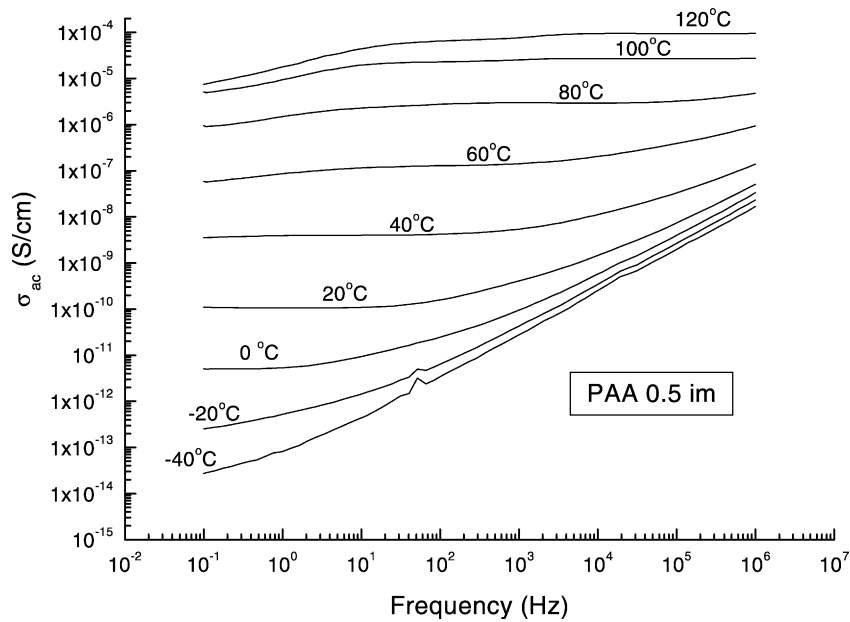


Fig. 5. σ_{ac} vs. frequency (Hz) for PAA0.5Im at various temperatures.

3.3. Conductivity measurement

The conductivity of thin films of the blends cast onto platinum electrodes was determined using impedance spectroscopy in the frequency range from 10^{-1} to 10^6 Hz and temperature range from 233 to 393 K. Figs. 5 and 6 displays the frequency dependence of the alternating current, ac conductivity (σ_{ac}) of PAA0.5Im and PAA1Im as a function of temperature. In both samples the curves comprise the frequency independent conductivity plateau regions, which are well developed at low frequencies and at low tempera-

tures and expand and shift toward higher frequencies with increasing temperature. The irregularities on low frequency side at higher temperatures, i.e. $T > 40^\circ\text{C}$ for both samples are caused by electrode polarization due to blocking effect of the platinum electrodes. The direct current, dc conductivity (σ_{dc}) of the samples is estimated from the ac conductivity plateaus. The plateau values in the medium-frequency range coincide well with dc conductivity values obtained from the Z' minimum in the real and imaginary (Z'/Z'') plot of impedance. Therefore, dc conductivities could be taken from the extrapolation of ac conductivity plateaus. The

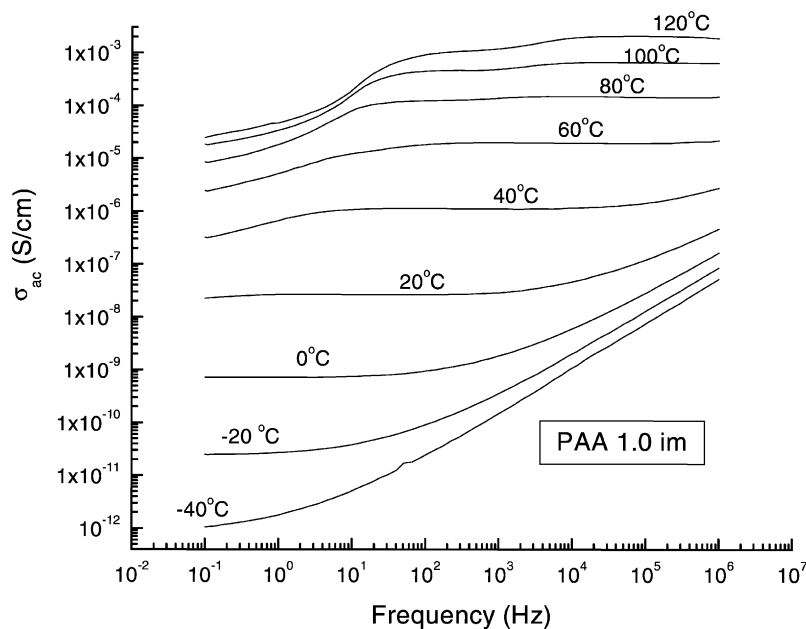


Fig. 6. σ_{ac} vs. frequency (Hz) for PAA1.0Im at various temperatures.

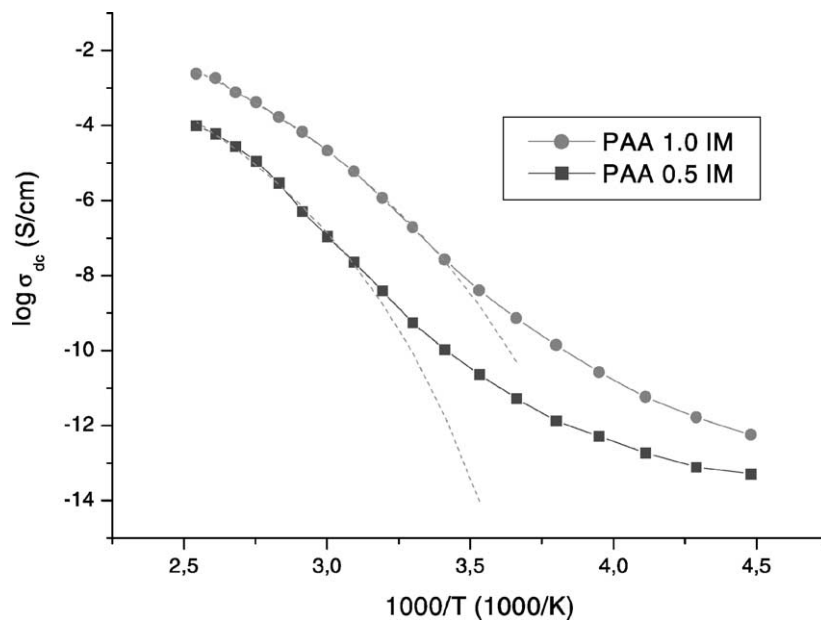


Fig. 7. Temperature dependence σ_{dc} of PAAxIm.

temperature dependence of the dc conductivities of $x = 0.5$ and 1.0 are compared in Fig. 7. A marked curvature is observed for the blends above their glass transition temperatures. Typical curves are interpreted with the Vogel–Tamman–Fulcher (VTF) equation (Eq. (1)) and this is verified by inserting the appropriate VTF fits into Fig. 7.

$$\sigma = \sigma_0 \exp\left(-\frac{B}{k(T - T_0)}\right) \quad (1)$$

where σ_0 is the pre-exponential factor, B and T_0 the temperature independent empirical parameters. T_0 is generally placed about 50 K below T_g and is idealized as the temperature at which all free volume vanishes. The T_0 values of $x = 0.5$ and 1 are 225 and 200 K, respectively. The conductivity of the blends exhibits less temperature sensitive behavior near T_0 , however, at higher temperatures conductivity increases with temperature. This may be due to onset of the segmental relaxations.

It was previously mentioned that the membrane materials based on carboxylic acid groups shows no significant proton conductivity even at higher level of hydration. Because $-\text{COOH}$ groups are less sensitive to hydrolysis and higher $\text{p}K_a$ values [13].

The intercalation of imidazol with different doping ratio, x into PAA as Brønstedt acid increased the conductivity PAAxIm membranes. The reason may be imidazol, like water, acts as proton donor and acceptor in the proton conduction process. In this sense it behaves amphoteric but with respect to other compounds they are more basic than water [9]. FT-IR of PAAxIm confirmed that imidazol is partially protonated from “free” nitrogen side. A Grotthuss type diffusion mechanism may explain the proton diffusion process within protonated and unprotonated heterocycles. Because the protonic defect may cause local disorder by forming

(...Him-(HimH⁺)-imH...) configuration as discussed in the literature [14]. The use of imidazol in a suitable acidic host polymer to increase the concentration of defect protons may also technological interest. Further systems like PAMPSA-imidazol are under investigation and will be communicated soon.

4. Conclusions

Novel blends from PAA and Im form amorphous and transparent films, which are thermally stable up to 200 °C. From FT-IR spectra it is evident that hydrogen bonds exist between protonated and unprotonated Im units. With increasing Im content the glass transition temperature decreases while their conductivity increase, reaching 10^{-3} S/cm at 120 °C. The proton migration may occur through movement of the proton vacancies that is a Grotthuss type diffusion mechanism. From the σ_{dc} isotherm it can be concluded that proton transport is controlled by the segmental motions of the polymer chains.

Acknowledgements

A. Bozkurt acknowledges the DAAD scholarship during his stay in Germany. The authors thank C. Sieber, A. Manhart, E. Muth and P. Rader for their technical assistance.

References

- [1] K.D. Kreuer, Th. Dippel, W.H. Meyer, J. Maier, Mat. Res. Soc. Symp. Proc. 29 (1993) 273–282.

- [2] J.C. Lassegues, J. Grondin, M. Hernandez, B. Maree, *Solid State Ionics* 145 (2001) 37–45.
- [3] G. Alberti, M. Casciola, *Solid State Ionics* 145 (2001) 3–16.
- [4] A. Bozkurt, W.H. Meyer, *Solid State Ionics* 138 (2001) 259–265.
- [5] M. Kawahara, J. Morita, M. Rikukawa, K. Sanui, N. Ogata, *Electrochim. Acta* 45 (2000) 1395–1398.
- [6] A. Bozkurt, M. Ise, K.D. Kreuer, W.H. Meyer, G. Wegner, *Solid State Ionics* 125 (1999) 225.
- [7] A. Bozkurt, W.H. Meyer, *J. Polym. Sci., Part B: Polym. Phys.* 39 (2001) 1987–1994.
- [8] V.Z. Bermudez, M. Armand, C. Poinignon, L. Abello, J.Y. Sanches, *Electrochim. Acta* 37 (1992) 1603–1609.
- [9] K.D. Kreuer, A. Fuchs, M. Ise, M. Spaeth, J. Maier, *Electrochim. Acta* 43 (1998) 1281–1288.
- [10] A. Schechter, R.F. Savinell, *Solid State Ionics* 147 (2002) 181–187.
- [11] M. Schuster, W.H. Meyer, G. Wegner, H.G. Herz, M. Ise, M. Schuster, K.D. Kreuer, J. Maier, *Solid State Ionics* 145 (2001) 85–92.
- [12] T. Otsu, L. Quach, *J. Polym. Sci., Polym. Chem. Ed.* 19 (1981) 2377–2389.
- [13] K.D. Kreuer, *Chem. Mater.* 8 (1996) 610–641.
- [14] W. Münch, K.D. Kreuer, W. Silvestri, J. Maier, G. Seifert, *Solid State Ionics* 145 (2001) 437–443.